AIAA JOURNAL
Vol. 45, No. 4, April 2007

Technical Notes

TECHNICAL NOTES are short manuscripts describing new developments or important results of a preliminary nature. These Notes should not exceed 2500 words (where a figure or table counts as 200 words). Following informal review by the Editors, they may be published within a few months of the date of receipt. Style requirements are the same as for regular contributions (see inside back cover).

Effect of Aspect Ratio on the End-Wall Flow of a Streamlined Cylinder

R. Rifki* and A. Ahmed†
Auburn University, Auburn, Alabama 36849
and
M. Javed Khan‡
Tuskegee University, Tuskegee, Alabama 36088

DOI: 10.2514/1.21642

Nomenclature

AR	=	aspect ratio, h/t
h	=	height of streamlined cylinder
Re	=	Reynolds number, $U_\infty t/\nu$
t	=	maximum thickness of the streamlined cylinder
U_∞	=	freestream velocity
u, v	=	streamwise and vertical velocity components
x, y, z	=	right-handed coordinate system with origin at the leading edge of the model
δ	=	boundary-layer thickness based on $u = 0.99U_\infty$
ν	=	kinematic viscosity
ξ	=	vorticity in the z direction, $(\frac{\partial v}{\partial x} - \frac{\partial u}{\partial y})\frac{t}{U_\infty}$

I. Introduction

THE flowfield around surface-mounted obstacles such as wings and other protuberances has been extensively investigated over the years. The interest in this configuration is due to its pervasive visibility in a variety of applications, for example, wing body, blade hub, submarine hull appendage, bridge piers, etc. The flowfield in the upstream region of this configuration is dominated by "secondary flow of the first kind," which is a consequence of streamlines curvature [1]. The physical presence of an obstacle imposes pressure gradient on a nominally two-dimensional approach boundary layer, which leads to the flow separation that is manifested in the form of a complex system of vortices commonly referred to as the "juncture-vortex system." The characteristics of this juncture-vortex system are Reynolds number dependent. Earlier investigations (Khan et al. [2]) documented distinct nature of this phenomenon in the form of regimes of static and dynamic system of vortices. The flowfield is also strongly influenced by geometric factors as well, including aspect ratio, leading-edge radius, and shape of attachment line of the obstacle. For example, Kawamura et al. [3] reported von Kármán vortex shedding from surface-mounted cylinders of aspect ratios larger than 4. They also observed an upwash towards the free end of the cylinder and the formation of trailing-edge vortices in addition to the juncture-vortex system. Similarly, Okamoto and Sunabashiri [4] observed an augmentation of downwash from the free end of a cylinder due to the juncture-vortex system for an aspect ratio less than 2. Based on the smoke flow visualization results, Thomas [5] reported an interesting phenomenon of the "splitting" of the juncture-vortex upstream of a surface-mounted cylinder; however, he did not offer any explanation for this splitting. Ahmed and Khan [6] made similar observations for surface-mounted swept wings and attributed this phenomenon to the attenuation and amplification of axial strains imposed on the vortices due to back and forward wing sweep, respectively.

Coupling between the end-wall flow and coherent structures in the wake of circular cylinders have also been documented in detail in the past, but have mainly focused on the vortex dislocation, streamwise vortices, and variations in the Strouhal number at subcritical Reynolds numbers [7–10]. Similarly, the influence of end conditions, that is, the role of juncture vortices on the two dimensionality of wakes is well established; however, very limited studies have focused on the effect of aspect ratio in the upstream region where the juncture vortices originate [11].

The adversity of pressure gradient in the juncture region, and therefore the location of primary singular point, largely depend on the amount of relaxation provided by the aspect ratio to the flow as it traverses around or above the obstacle. The present investigation was undertaken with the objective of documenting in detail the physics of flow and characteristics of the juncture-vortex system of a surface-mounted wing with aspect ratios varying from $\frac{1}{2}$ to 8.

II. Experimental Setup

Tests were conducted in the Auburn University 45×45 cm cross section test section water tunnel capable of continuously variable speed from 0–1 m/s in open and closed surface operations. The test model was made from 44 mm thick high-density black polyurethane with an overall length of 302 mm, a round nose, and tapered trailing edge as shown in Fig. 1.

The streamlined cylinder geometry was selected to eliminate the periodicity induced by the von Kármán vortices in the wake. The models were machined in different heights and stacked vertically to achieve an aspect ratio of up to 8. The basic wing model (aspect ratio of $\frac{1}{2}$) was attached to the boundary layer plate directly, with the leading edge of the model located at 70 cm from the leading edge of the boundary layer plate. Remaining sections were secured on top of this base with screws and pins. The 2.5 m long and 19 mm thick boundary layer plate had a 1:8 fineness ratio elliptical leading edge and a tapered trailing edge. The plate was equipped with dye injection slot located at 13 cm from the leading edge of the plate for near-wall flow visualization. The same slot was later used for injection of seeds for particle image velocimetry (PIV) measurements. The schematic of the test setup and coordinate system used in this investigation is shown in Fig. 2.

During the preliminary flow visualization tests it was observed that the convection of turbulent spots introduced significant amount

Presented as Paper 4848 at the 23rd AIAA Applied Aerodynamics Conference, Toronto, Canada, 6–9 June 2020; received 7 December 2005; revision received 14 August 2006; accepted for publication 16 December 2006.

*Graduate Research Assistant, Aerospace Engineering Department. Student Member AIAA.
†Associate Professor, Aerospace Engineering Department. Associate Fellow AIAA.
‡Associate Professor, Aerospace Science Engineering Department. Senior Member AIAA.

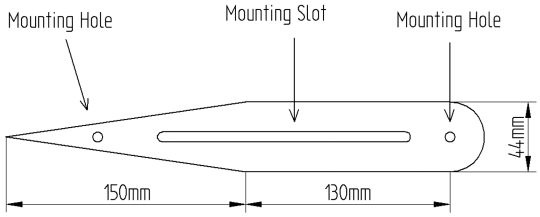

Fig. 1 Details of the model tested.

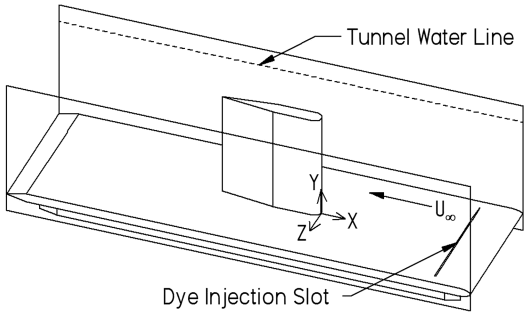

Fig. 2 Details of the experimental setup.

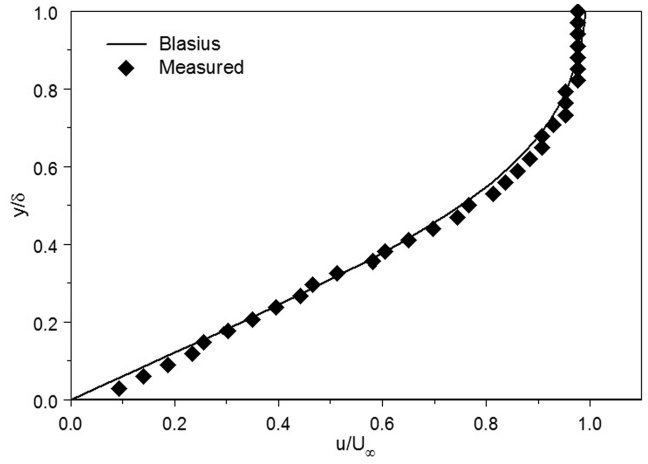

Fig. 3 Boundary layer profile.

of unsteadiness in the juncture region. The largest freestream velocity at which the turbulent spots were not observed was selected as the test speed. For this condition ($U_\infty = 50$ mm/s) the Reynolds number based on maximum thickness of the wing was 2000. Freestream turbulence intensity was measured to be less than 3.6%. Laminar boundary layer profile measured at a streamwise station where the leading edge of the model was later located is presented in Fig. 3. Deviation of the measured profile from Blasius profile is due to setting of the boundary layer plate at a slightly negative angle of attack to ensure attachment of the flow on the top surface. The boundary layer thickness was measured to be 27 mm. Integral quantities calculated from the measured boundary layer profile yielded a displacement thickness of 9 mm and a momentum thickness 4 mm for the present test conditions.

The near-wall flow was visualized with laser-induced fluorescence of sodium fluorescein salt injected in the boundary layer from a dye injection slot. Location of primary singular point was measured from video records using image analyses tools in MatLab environment. The vortical structures in the flowfield were investigated using a hydrogen bubbles probe consisting of three platinum wires strung at different heights. The probe was connected to 2-DOF traversing system for precise axial and vertical positioning of the bubble wires. Size and quantity of hydrogen bubbles was fine tuned for flow visualization by adjusting the applied voltage (12–60 V). Bubbles were illuminated in the plane of symmetry of the model with a laser light sheet made from a 5 W Argon Ion laser and OZ optics fiber optic light sheet generator. A Sony CCD camera was used to make video records.

PIV measurements in the plane of symmetry were made with Dantec Dynamics Flow Map system consisting of 50 mJ dual-pulsed YAG lasers and 1.1×1.1 k cross-correlation camera. The interrogation region was 32×32 pixels with a 50% overlap. The resulting vector spacing was 0.8 mm. Flow statistics were determined using 30 pairs of images. Uncertainty in the measured values of the mean velocities was calculated to be less than 2%. Vorticity contours and streamlines were generated using TecPlot software. At few select locations, PIV data was also validated with the help of hot film anemometry.

III. Results and Discussion

Flow visualization results confirmed the presence of a static system of vortices consisting of three corotating vortices and accompanied by two counterrotating flow structures (hereafter referred to as foci structures) that originate from the wall due to vortex-wall interaction. The foci structures observed during the present investigation were similar to those reported by Khan et al. [2] for static system of vortices. Hydrogen bubbles marking the vortex system for aspect ratios of $\frac{1}{2}$ and 8 presented in Fig. 4 show the contrasting flow away from the plate surface for AR $= \frac{1}{2}$ compared to the more inward flow for AR $= 8$ case. It was observed that with an increase in the aspect ratio, there was more entrainment of fluid due to inflow, and consequently the bifurcation streamline (discussed later) displaced vertically upward along the attachment line and the primary vortex (vortex closest to the leading edge) moved upstream. These observations were later confirmed by the PIV measurements.

Velocity vectors calculated from PIV measurements in the plane of symmetry of the cylinder of aspect ratio $\frac{1}{2}$ and 8 are shown in Fig. 5.

In addition to the primary vortices (streamwise position marked by a symbol ▲ on horizontal axis) visible in the flow visualization results of Fig. 4, Fig. 5 also shows the presence of the bifurcation streamline (location marked by a symbol ▷ on vertical axis) at approximately $y/t = 0.38$ for AR $= \frac{1}{2}$. The bifurcation streamline divides the juncture flow into an inward flow that moves towards the corner and an outward flow. The inward flow is also responsible for

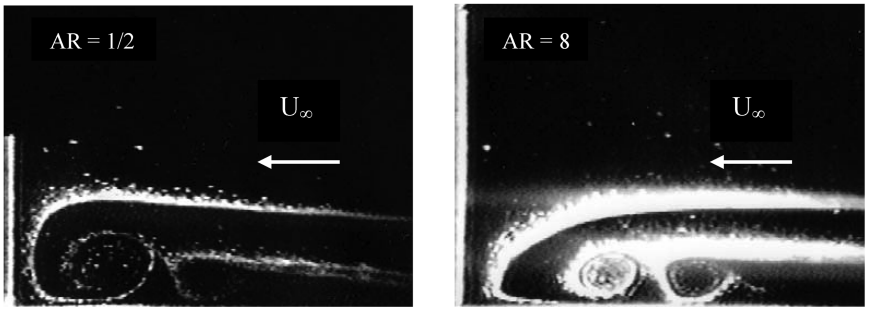

Fig. 4 Hydrogen bubbles marking the juncture-vortex system in the plane of symmetry.

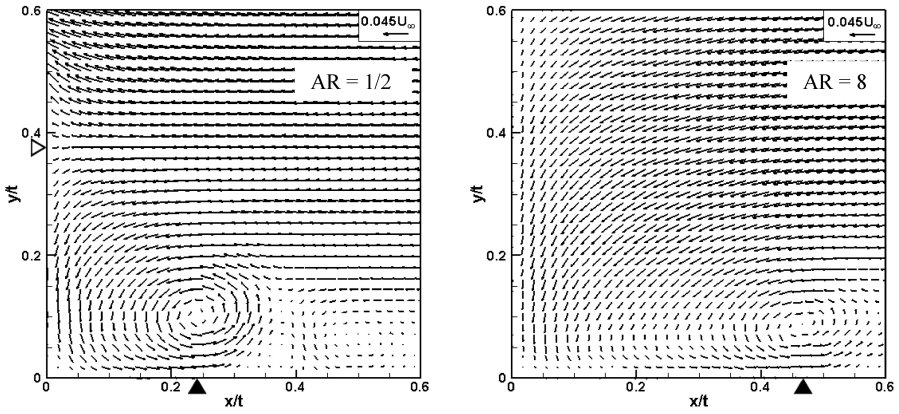

Fig. 5 Velocity vectors plot in the plane of symmetry of AR $= \frac{1}{2}$ and AR $= 8$ cylinders: ▷, bifurcation streamline; ▲, primary vortex.

the entrainment of external fluid in the corner region and consequently the reversed flow that strongly influences the streamwise pressure gradient and the location of primary singular point. The height of the bifurcation streamline was observed to vary directly with the aspect ratio moving from approximately $y = 2/3\delta$ for AR $= \frac{1}{2}$ to $y = 2\delta$ for AR $= 1\frac{1}{2}$ case. The bifurcation streamlines could not be observed from the vector plots for higher aspect ratios, as it was outside the measurement region; however, the hydrogen bubble wire positioned at different vertical distances validated the overall trends.

Plots of streamlines covering the range of aspect ratios investigated are presented in Fig. 6 and show that the size and location of the primary vortex was strongly influenced by the cylinder aspect ratio. For up to AR $= 4$, the primary and secondary vortices were observed to move upstream along with the strengthening of foci structures. This was followed by the movement of vortex system toward the leading edge of the cylinder and large inflow due to upward displacement of the bifurcation streamline.

In presenting the data it was observed (and supported by dimensional argument) that a more consistent trend was observed when the local height h of the cylinder was used instead of its thickness for scaling. The nondimensional streamwise locations (x/h) of the primary and secondary vortices plotted in Fig. 7 show that although the distance of the vortices from the cylinder attachment line reduced with increasing aspect ratio, the reduction for the secondary vortex was more rapid. This is attributed to an increased interaction between the vortical structures and the wall. It is also clearly evident from Fig. 7 that for AR > 4 the streamwise locations of the primary and secondary vortices became less sensitive to changes in aspect ratio. Furthermore, the streamwise distance between the two vortices rapidly reduced and approached an asymptotic state for AR > 4.

The influence of aspect ratio on the size of the system can be observed in Fig. 4. However, flow visualization of vortical structures can be influenced by the location of the bubble generating wire probes and subsequent quantity and size of the entrained bubbles. PIV measurements were therefore used to calculate vorticity to quantify the influence of aspect ratio. Presented in Fig. 8 are the maximum and minimum vorticity measured in the plane of symmetry flow. The positive vorticity corresponds to the primary

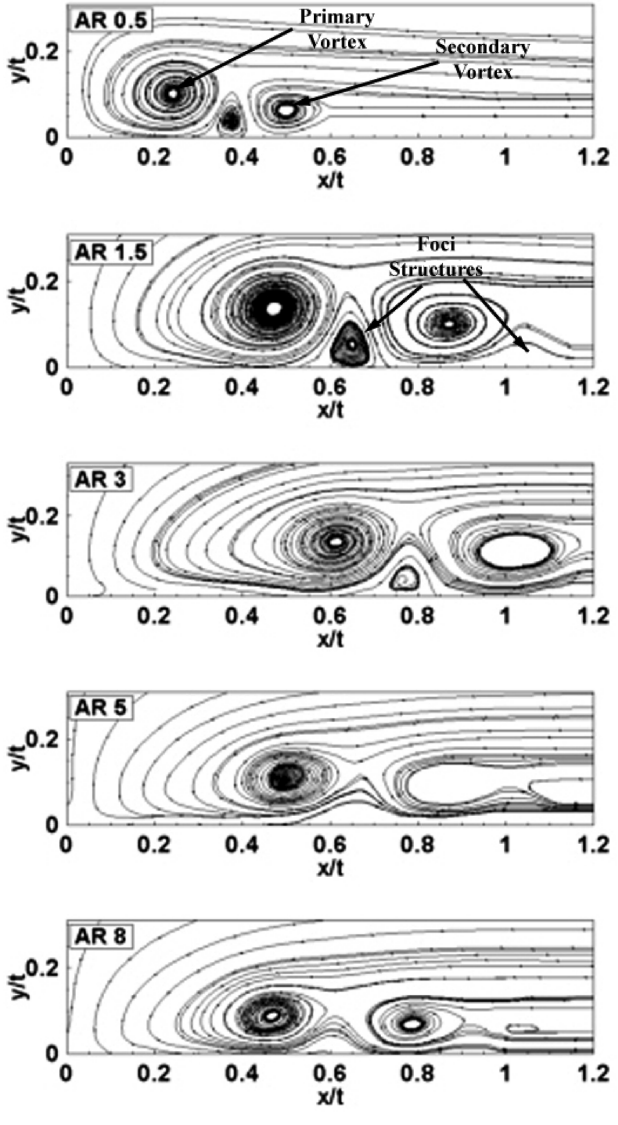

Fig. 6 Streamlines in the plane of symmetry.

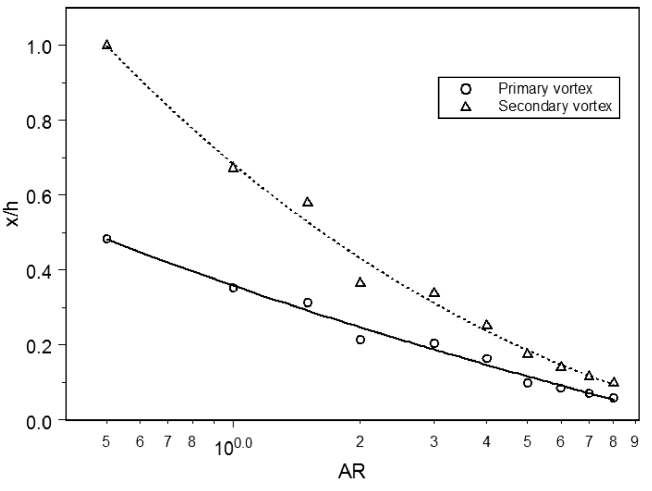

Fig. 7 Streamwise location of primary and secondary vortices.

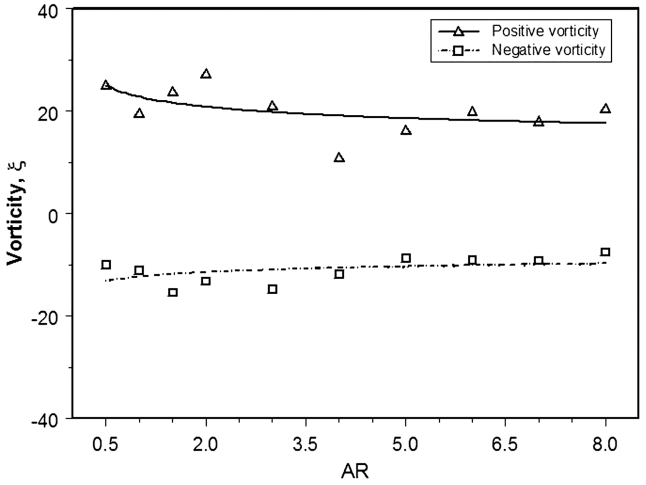

Fig. 8 Maximum positive and negative vorticity in the plane of symmetry.

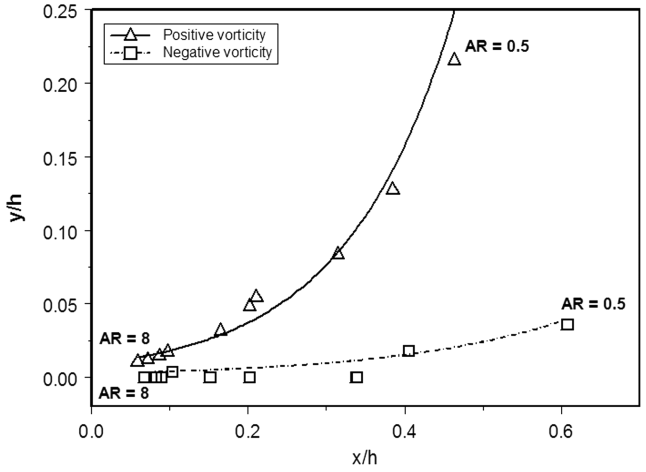

Fig. 9 Trajectory of maximum and minimum vorticity.

vortex and negative vorticity is due to the first counterrotating foci structure that resides between the primary and secondary vortices (Fig. 6). A strengthening of the primary vortex was observed for $AR = 2$. In fact for this aspect ratio, the vortex system had the maximum positive vorticity which is indicative of axial stretching. Further increase in aspect ratio resulted in reduction in the vorticity due to a combination of vorticity diffusion and wall interaction, with $AR = 4$ having the minimum positive vorticity. A slight increase in vorticity was observed in the vortex system with further increase in aspect ratio. Negative vorticity concentrated in the foci structure followed similar trends. The mean lines passing through the data suggest that the vortex strengths lose dependency on aspect ratio for $AR > 6$.

The trajectory of maximum and minimum vorticity points in the plane of symmetry presented in Fig. 9 clearly show that for increasing aspect ratio the primary vortex moves towards the wall, and the counterrotating foci structure embeds almost underneath it and is confined to the wall. This is attributed to the higher inflow due to vertical displacement of the bifurcation streamline. The wallward migration of the primary vortex is similar to the juncture-vortex trajectory for higher Reynolds number [2]. A consequence of this behavior is the production of high wall shear stresses that also explains the "scrapping" of flow visualization dye in the junction region of high-aspect-ratio wings reported in the past [6].

IV. Conclusions

Aspect ratio strongly influences the flow in the juncture region of a surface-mounted obstacle. With increasing aspect ratio the location of bifurcation streamline displaced vertically upwards along the attachment line. The primary and secondary vortices approached each other and formed closer to the cylinder leading edge. For $AR > 4$ the distance between the primary and secondary vortices became insensitive to further increase in aspect ratio. Vorticity in the plane of symmetry approached a uniform value for $AR > 6$. Trajectories of maximum and minimum vorticity points showed a stronger kinematic interaction of vortices with their mirror images in the wall. Furthermore, it is concluded that for aspect ratios greater than 6 the vortex system was no longer influenced by this parameter.

References

[1] Prandtl, L., *Essentials of Fluid Dynamics*, Blackie & Sons, Glasgow, Britain, 1952.

[2] Khan, M. J., Ahmed, A., and Trosper, R. J., "Dynamics of the Juncture Vortex," *AIAA Journal*, Vol. 33, No. 7, 1995, pp. 1273–1278.

[3] Kawamura, T., Hiwada, M., Hibino, T., Mabuchi, I., and Kumada, M., "Flow Around a Finite Cylinder on a Flat Plate," *Bulletin of the JSME*, Vol. 27, No. 232, 1984, pp. 2142–2151.

[4] Okamoto, S., and Sunabashiri, Y., "Vortex Shedding from a Circular Cylinder of Finite Length Placed on a Ground Plane," *Journal of Fluids Engineering*, Vol. 114, No. 4, 1992, pp. 512–521.

[5] Thomas, A. S. W., "The Unsteady Characteristics of Horseshoe Vortex System," *Physics of Fluids*, Vol. 30, No. 2, 1987, pp. 283–283.

[6] Ahmed, A., and Khan, M. J., "Effect of Sweep on Wing-Body Juncture Flow," AIAA Paper 95-0868, Jan. 1995.

[7] Slaaouti, A., and Gerrard, J. H., "An Experimental Investigation of the End Effects on the Wake of Circular Cylinders Towed Through Water at Low Reynolds Numbers," *Journal of Fluid Mechanics*, Vol. 112, Nov. 1981, pp. 297–314.

[8] Eisenlohr, H., and Eckelmann, H., "Vortex Splitting and its Consequences in the Vortex Street Wake of Cylinders at Low Reynolds Numbers," *Physics of Fluids A*, Vol. 1, No. 2, 1989, pp. 189–192.

[9] Williamson, C. H. K., "Oblique and Parallel Modes of Vortex Shedding in the Wake of a Cylinder at Low Reynolds Numbers," *Journal of Fluid Mechanics*, Vol. 206, Sept. 1989, pp. 579–627.

[10] Stager, R., and Eckelmann, H., "The Effect of Endplates on the Shedding Frequency of Circular Cylinders in the Irregular Range," *Physics of Fluids A*, Vol. 3, No. 9, 1991, pp. 2116–2121.

[11] Farivar, D., "Turbulent Uniform Flow Around Cylinders of Finite Length," *AIAA Journal*, Vol. 19, No. 3, 1981, pp. 275–281.

J. Gore
Associate Editor